Int. J. Solids Structures. Vol. 11, pp. 347–355. Pergamon Press 1975. Printed in Great Britain

COMPUTATION OF INCREMENTAL TORSIONAL PLASTIC WAVES WITH RATE-DEPENDENT MODELS

A. K. BANERJEE†
Northrop Technical Services, Inc. P.O. Box 1484, Huntsville, Alabama 35807, U.S.A.

and

L. E. MALVERN‡
Center for Dynamic Plasticity, Department of Engineering Sciences, 231 Aero Building, University of Florida, Gainesville, Florida 32611, U.S.A.

(*Received* 1 *April* 1974; *revised* 22 *July* 1974)

Abstract—A theoretical analysis of the experimental data of Yew and Richardson on incremental plastic waves in copper is given. Three different strain-rate-dependent constitutive models are considered, and each is integrated by a different numerical scheme. Results show that the intermediate level strain data can be fairly well explained by any one of these models. Good match between the theory and the experiment has, however, not been obtained for the very low and the large amplitude strains. A rate-independent solution is presented for contrast, and it shows consistently poor agreement with the experiment.

INTRODUCTION

Yew and Richardson [1] published an experimental study of the strain-rate sensitivity of copper and its effect on the velocity of propagation of shearing strain. Thin-walled tubes of copper were loaded in torsion to eliminate the effects of radial inertia. Tests with prestressed specimens showed that while large strains propagated with speeds given by a rate-independent theory, lower level strains traveled faster than predicted by such a theory. It was concluded that this discrepancy must be due to the strain-rate sensitivity of copper.

The purpose of the present paper has accordingly been to analyze these experimental data in the light of a strain-rate-dependent theory of inelastic wave propagation. Three different nonlinear constitutive models, of the types proposed earlier in the literature on dynamic plasticity, have been examined. The attempt to choose the parameters in these constitutive models for a reasonable match between the theory and the experiment gave rise to the mathematical problem of convergence of the numerical solutions. The problem was solved by using more powerful numerical methods as the situation warranted. Thus the Malvern [2] linear overstress model was solved by Bianchi's [3] scheme, the Cristescu [4] model by the second-order Courant, Isaacson, Rees scheme developed by Ranganath and Clifton [5], and Perzyna's [6] exponential overstress version of Malvern's model by developing an integro–differential approach. Comparison of these numerical solutions was made with the experimental data and with a rate-independent solution based on a bilinear stress–strain curve. It was found that intermediate level strain data are fairly well represented by any one of the rate-dependent models, while the very low and large amplitude strains are not well reproduced. The exponential overstress model was inferior to the other two

†Senior Engineer, Dynamics
‡Professor.

rate-dependent models, at least with the parameter values used. The rate-independent solution, on the other hand, gives consistently poor results.

BASIC EQUATIONS

The basic equations of motion and compatibility are

$$\frac{\partial \tau}{\partial x} = \rho \frac{\partial v}{\partial t} \tag{1}$$

$$\frac{\partial v}{\partial x} = \frac{\partial \gamma}{\partial t}, \tag{2}$$

where τ and γ are the shear stress and strain (engineering definition) and v is the particle velocity in the tangential direction. It may be noted that these equations are exact even for large strains.

CONSTITUTIVE EQUATIONS

The following three constitutive models are examined in turn.

(i) Linear overstress model, Malvern[2],

$$\frac{\partial \gamma}{\partial t} = \frac{1}{G}\frac{\partial \tau}{\partial t} + \frac{k}{G}[\tau - f(\gamma)]. \tag{3}$$

Here G is the shear modulus, k is the rate-sensitivity parameter and $f(\gamma)$ is the dynamic relaxation boundary in the stress–strain plane.

(ii) Exponential overstress model, Perzyna[6],

$$\frac{\partial \gamma}{\partial t} = \frac{1}{G}\frac{\partial \tau}{\partial t} + \frac{k}{G}\left[\exp\left(\frac{\tau - f(\gamma)}{A}\right) - 1\right]. \tag{4}$$

Here k and A represent the two rate-sensitivity parameters in this model.

(iii) Quasilinear model, Cristescu[4],

$$\frac{\partial \gamma}{\partial t} = \left[\frac{1}{G} + \phi(\tau, \gamma)\right]\frac{\partial \tau}{\partial t} + \frac{k}{G}[\tau - f(\gamma)]. \tag{5}$$

Here the term $\phi(\tau, \gamma)\ (\mathrm{d}\tau/\mathrm{d}t)$ accounts for any instantaneous inelastic response and was introduced in the literature on purely phenomenological grounds (see, e.g. Ref. [7]). As such, the procedure for determining a suitable form of this function is rather empirical. Thus Cristescu[4] chose a simple function as a first approximation to the curve for instantaneous stress–strain behavior, and subsequent adjustment was necessary for a good fit to the strain–time curve up to its inflection point. The basic form chosen in the present investigation is the parabola $\tau = B(\gamma + \gamma_1)^{1/2}$ where B and γ_1 are constants to be determined. The instantaneous response curve is obtained from Eq. (5) as

$$\mathrm{d}\gamma = \left[\frac{1}{G} + \phi(\tau, \gamma)\right]\mathrm{d}\tau, \tag{6}$$

and its slope is set equal to that of the parabola chosen. Thus

$$\frac{1}{G} + \phi(\tau, \gamma) = \left(\frac{2}{B}\right)(\gamma + \gamma_1)^{1/2}. \tag{7}$$

B and γ_1 are evaluated by requiring that the initial slope is the elastic modulus and that the instantaneous stress–strain curve passes through the initial yield point. Eq. (7) thus gives the first approximation as

$$\phi + \frac{1}{G} = 2[\{\gamma - \gamma_0 + (\tau_0/2G)\}/2G\tau_0]^{1/2}. \tag{8}$$

For subsequent adjustment for a good fit to the strain–time data, an additional parameter α was introduced multiplying $\gamma - \gamma_0$ in Eq. (8), which then takes the form given in Eq. (9). The value of $\alpha = 1500$ was finally used in the computation.

$$\phi + \frac{1}{G} = 2\left[\left(\frac{\alpha}{2G\tau_0}\right)(\gamma - \gamma_0) + \left(\frac{1}{4G^2}\right)\right]^{1/2} \tag{9}$$

Eq. (9) would correspond to an instantaneous curve

$$\Delta\tau = \left[\left(\frac{2G\tau_0}{\alpha}\right)\Delta\gamma + \left(\frac{\tau_0}{\alpha}\right)^2\right]^{1/2} - \left(\frac{\tau_0}{\alpha}\right)$$

relating incremental stress $\Delta\tau$ and incremental strain $\Delta\gamma$. It is emphasized that there is no intention to imply that any finite-amplitude instantaneous loading would actually follow this curve. The reciprocal of $\phi + (1/G)$ is the slope of the instantaneous curve. According to Eq. (9) the slope would approach zero for large values of $\gamma - \gamma_0$, which is not reasonable; hence the slope given by Eq. (9) should be regarded as at best the leading term (dominant for small $\gamma - \gamma_0$) of a representation of $[\phi + (1/G)]^{-1}$.

RELAXATION BOUNDARY AND ELASTIC MODULUS

The quasistatic stress–strain curve given by Yew and Richardson for cold-worked copper was essentially linear in the plastic region covered by the experiments. For the calculations, a linear dynamic relaxation boundary was assumed of the form

$$\tau - \tau_0 = G_t(\gamma - \gamma_0) \tag{10}$$

where (τ_0, γ_0) is the initial stress–strain point and G_t is the tangent modulus. For the computations the numerical value $G_t = 66{,}000$ psi was used; this is consistent with the value of finite-amplitude plastic wave speed $c_p = 8700$ in./sec, estimated from the graphical data presented by Yew and Richardson, and a density $\rho = 8{\cdot}71 \times 10^{-4}$ lb-sec^2/in.^{4}. The dynamic elastic modulus was taken as $G = 6 \times 10^6$ psi, corresponding to the reported elastic shear wave speed of 83,000 in./sec.

INTERIOR DIFFERENTIAL EQUATIONS

The general form

$$\frac{\partial\gamma}{\partial t} = \left[\frac{1}{G} + \phi(\tau, \gamma)\right]\frac{\partial\tau}{\partial t} + \psi(\tau, \gamma) \tag{11}$$

reduces to Eqs. (3), (4) or (5) with appropriate choices of ϕ and ψ. The interior differential equations are

$$d\tau \mp \rho c\, dv = -\rho c^2 \psi\, dt \tag{12}$$

along the characteristics defined by

$$dx = \pm c\, dt, \text{ where } c = 1\Big/\left[\rho\left(\frac{1}{G}+\phi\right)\right]^{1/2}. \tag{13}$$

BOUNDARY AND INITIAL CONDITIONS

Yew and Richardson[1] report strain–time data for three strain gage stations at 0·38, 1·50 and 2·75 in. from the impact end. The boundary condition for the numerical solutions was taken to be the incremental strain–time record for the first strain gage (at 0·38 in.). The incremental stress–strain behavior is independent of the initial point, with the linear dynamic relaxation boundary of Eq. (10), for the linear and exponential overstress models. The function ϕ given by Eq. (9) contains the value of τ_0 only in the combination α/τ_0. Hence the same incremental behavior for a different τ_0 would require a different α for the quasilinear model. The calculations were made with $\tau_0 = 10{,}440$ psi and $\gamma_0 = 0{\cdot}01$. The initial values were not given in [1], but the incremental behavior presented here does not require those values.

NUMERICAL SCHEMES

(i) Linear overstress model—Diamond-shaped meshes were used. The algorithm was the same as that given by Bianchi[3]. Because of the linear plastic stress strain function assumed, simple elimination of variables is possible. Computation time was of the order of seconds.

(ii) Perzyna model—The presence of the exponential function in Eq. (4) caused the integration scheme at the boundary to be very sensitive to any waviness of the numerical data that remained after interpolation and smoothing. Also, solution of the interior differential equations written in implicit difference form required uneconomically small step sizes when the parameters were chosen to represent a material with only slight rate-sensitivity as in the present case. The integro–differential approach discussed in the following has the advantage that, while the integration operation takes care of any rough boundary data, the convergence process itself is very much improved by a direct elimination of one of the variables.

Consider Eq. (4). For a fixed material point, i.e. constant x, this nonlinear ordinary differential equation can be given a variation-of-parameter solution as

$$\tau = G(\gamma - \gamma_0) + k(t - t_0) + \mu(t), \tag{14}$$

where γ_0 is the strain at time t_0. Substituting Eq. (14) in Eq. (4) written as an ordinary differential equation and solving the resulting differential equation gives

$$\mu(t) = -A \ln\left[\exp\left(-\frac{\tau_0}{A}\right) + \frac{k}{A}\int_{t_0}^{t} \exp\left(\frac{1}{A}[G(\gamma(s)-\gamma_0) + k(s-t_0) - f(\gamma(s))]\right) ds\right], \tag{15}$$

where τ_0 is the stress at t_0. With

$$g(s) = \frac{1}{A}[G(\gamma(s)-\gamma_0) + k(s-t_0) - f(\gamma(s))] \tag{16}$$

and

$$\psi = k(t - t_0) - \tau_0 - A \ln\left[e^{-\tau_0/A} + \frac{k}{A}\int_{t_0}^{t} e^{g(s)}\,ds\right], \tag{17}$$

Eq. (14) is rewritten as

$$\tau = G(\gamma - \gamma_0) + \tau_0 + \psi. \tag{18}$$

On using Eq. (18) in Eq. (1) we obtain the following integro–differential equation

$$-G\frac{\partial \gamma}{\partial x} + \rho\frac{\partial v}{\partial t} = \frac{\partial \psi}{\partial x} \tag{19}$$

where ψ is given by Eq. (17). The expression for $(\partial\psi/\partial x)$ contains within the integral sign the term $(\partial\gamma/\partial x)$, but any discontinuous derivative that this may represent gets smoothed out upon integration. Thus Eqs. (19) and (2) may be looked upon as a set of quasilinear hyperbolic partial differential equations. The corresponding interior differential equations are

$$dv \mp c_2\,d\gamma = \frac{1}{\rho c_2}\frac{\partial \psi}{\partial x}dx \tag{20}$$

valid along the lines

$$dx = \pm c_2\,dt, \quad \text{where} \quad c_2 = (G/\rho)^{1/2}. \tag{21}$$

The numerical integration of equations (20) is carried out in the characteristic field of Fig. 1(a), where the associated mesh configurations are also indicated. To evaluate the quantity $(\partial\psi/\partial x)$, the solution has to be known at the point M on the line parallel to the x-axis. The integral

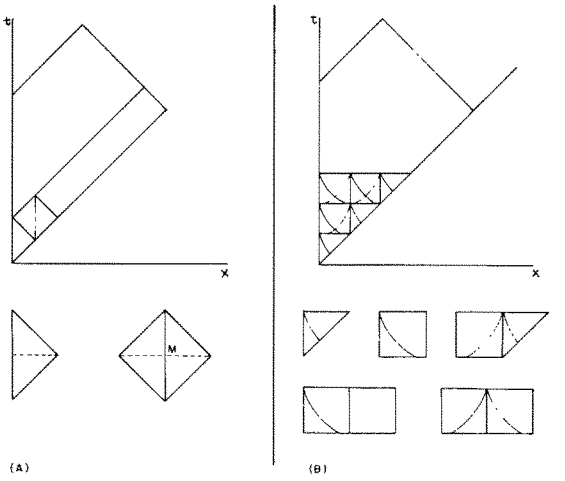

Fig. 1. Characteristics field and mesh configurations used for (A) exponential overstress model, (B) quasilinear model.

occurring in the expression for ψ, Eq. (17), is evaluated by the trapezoidal rule for each x-station considered. To prevent the integrand from exceeding the largest number that can be handled by the computer, e^{174} with the machine used, a recursive scheme of integration is developed (see Banerjee[8]). Computations with a step size of 1·1422 μsec and for a loading duration of 370 μsec required a machine time of 2·7 min on an IBM 360/65 computer.

(iii) Quasilinear Model—Computations for the quasilinear set of equations (1), (2), (5) were done by the second-order Courant, Isaacson, Rees method developed by Ranganath and Clifton[5]. One modification was found necessary in that a maximum of up to five additional iterations on the second order solutions had to be used. A sketch of the characteristics field and the mesh types involved is given in Fig. 1(b). Details of the computations scheme, which required using a "crossing routine," see Cristescu[9], when successive iterations oscillated about the relaxation boundary, are given in Banerjee[8]. With a step size of 0·5711 μsec, the computation time was 7·6 min on an IBM 360/65 machine for an impact duration of 370 μsec.

RESULTS

Figures 2–4 show the results of computations based on the linear overstress[2], exponential overstress[6] and quasilinear[4] models respectively. In each figure the experimental data of Yew and Richardson[1] and a rate-independent solution based on the bilinear quasistatic stress–strain curve are also presented.

Figure 2 shows the results for the linear overstress model (Eq. 3), with $k = 8{\cdot}5 \times 10^6$ sec^{-1}. It is seen that the rate-dependent solution gives in general a better description of the experimental response than the rate-independent solution. Incremental strain data below 0·04 per cent and above 1·0 per cent are not matched by the solution presented.

Figure 3 shows the results based on the exponential overstress model Eq. (4), with $k = 10^9$ psi sec^{-1} and $A = 250$ psi. Increasing k and/or decreasing A would give a solution showing less rate effect and better agreement with the experiments. However, even for the present values of k and A, the integral involved for evaluating ψ (Eq. 17) has to be broken down into thirteen parts, and a solution showing less rate effect can only be obtained at the expense of making the program more unwieldy. Even so, the present rate-dependent solution is closer to the experimental data than the rate-independent solution.

Solution for the quasilinear model, Eq. (5), is presented in Fig. 4. The overall agreement between this rate-dependent solution and the experimental response is probably the best among the

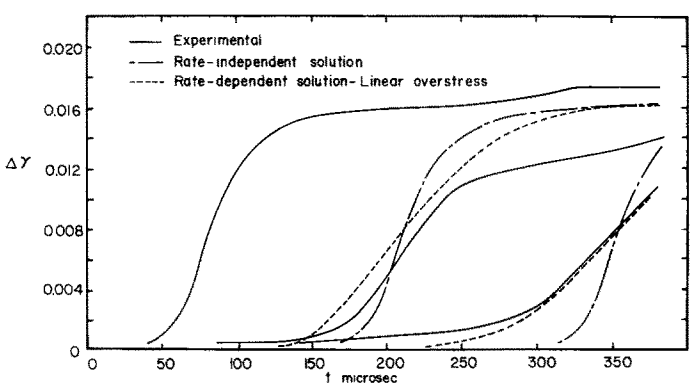

Fig. 2. Incremental strain–time plots for the linear overstress model at 0·38, 1·50 and 2·75 in. from impact end. First curve (0·38 in.) is taken as input for the calculations.

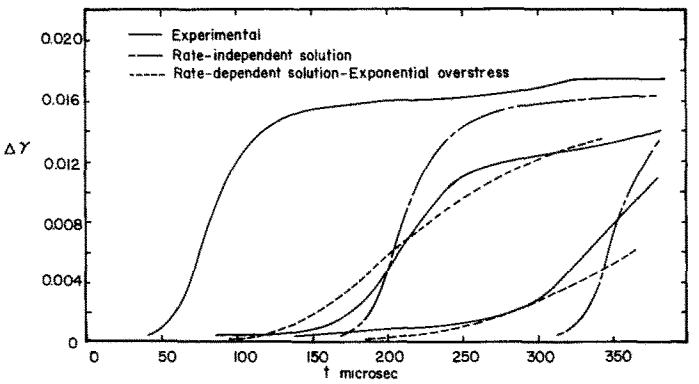

Fig. 3. Incremental strain–time plots for the exponential overstress model at 0·38, 1·50 and 2·75 in. from impact end. First curve (0·38 in.) is taken as input for the calculations.

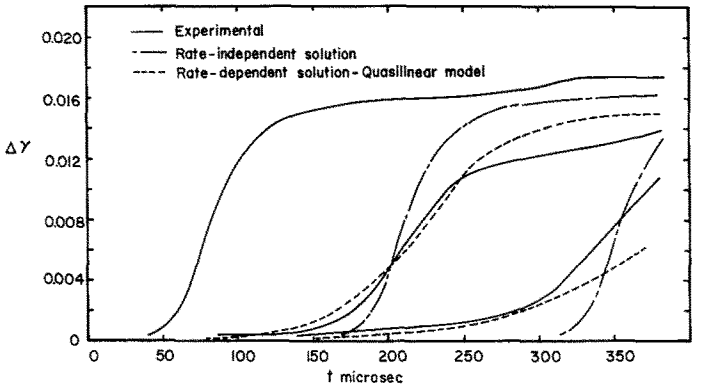

Fig. 4. Incremental strain–time plots for the quasilinear model at 0·38, 1·50 and 2·75 in. from impact end. First curve (0·38 in.) is taken as input for the calculations.

three models considered. It was seen that changing α in Eq. (9) has the effect of controlling the strain–time curve below the inflection point, while changing k in Eq. (5) controls the "lift" of the curve above the inflection. Similar observations were also made by Cristescu[4].

Even better agreement with the experimental results could probably have been obtained by further adjustment of the parameters of the quasilinear model. Further refinement was, however, not considered worthwhile until more experimental data is available for a variety of incremental loadings of the same material.

Figure 5 shows a stress–time plot at the boundary for the three constitutive models, together with the rate-independent solution, i.e. the quasistatic stress–strain values. It is seen that all the three rate-dependent solutions show a slight overstress initially when the strain-rate is high, but the relaxation boundary—quasistatic stress–strain relation as assumed in this case—is reached whenever the strain-rate becomes very small.

COMPARISON OF THE THREE MODELS AND NUMERICAL METHODS

The rate-independent solution plotted in Figs. 2–4 shows that the smaller strains propagated faster in the experiment than predicted by this theory, while the situation is reversed for large

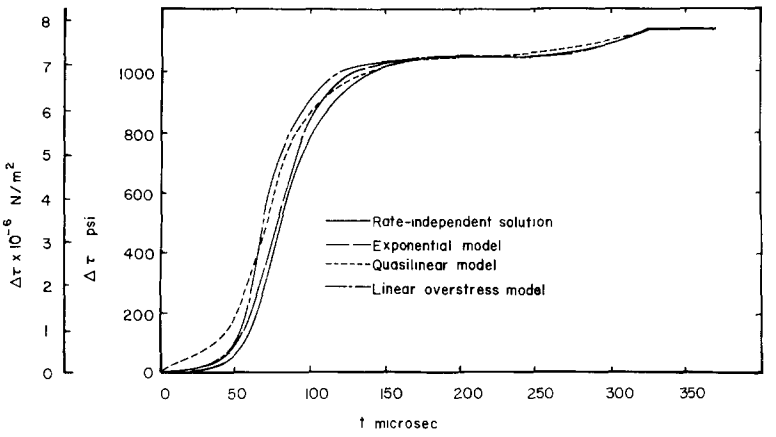

Fig. 5. Incremental stress–time plot at the boundary.

strains. This is the typical indication of strain-rate effects, as observed by Malvern [2]. Thus it is no surprise that the three models showed better agreement with the experiment than the rate-independent solution. The difference between the three rate-dependent solutions is evidently a consequence of the different constitutive models. The quasilinear model of Cristescu [4] seems to be better suited for describing the rate effects demonstrated in the experiments. One interesting thing to note is that the speed of propagation of any given level of strain is not well predicted by any one of the rate-dependent or rate-independent theories considered.

In terms of the numerical methods used, Bianchi's [3] algorithm seems to be the most appropriate to apply for a linear constitutive equation like the Malvern model for a linear relaxation boundary function. The second order accurate difference method of Ranganath and Clifton [5], when used with provisions for more iterations if required, seems to be a powerful tool for the more difficult quasilinear system.

The integro–differential scheme presented in this paper has the twin advantages of superior stability together with a suitability for handling rough boundary data. To give a relative estimate of stability, a Gauss–Seidel iteration on the implicit difference form of the characteristic relations for the Perzyna [6] model could admit parametric values up to about $k = 3 \times 10^8$ psi sec^{-1} and $1/A = 0{\cdot}001$ psi^{-1} for a step size of $0{\cdot}5711$ μsec—while the integro–differential method permitted the use of values such as $k = 10^9$ psi sec^{-1} and $1/A = 0{\cdot}004$ psi^{-1} for a step size twice as large.

CONCLUSIONS

(1) Three different rate-dependent constitutive equations were used to describe the incremental strain data in torsional impact obtained by Yew and Richardson [1]. Reasonable agreement was achieved with each of these models at the intermediate level strains but not at high and low levels. The quasilinear model gave somewhat better agreement than the others, and all three rate-dependent models gave better overall agreement than did a rate-independent solution based on the quasistatic stress–strain behavior.

(2) An integro–differential method of solution was presented for semilinear partial differential equations. Besides being inherently able to handle non-smooth boundary data, the method has stability characteristics superior to that of Gauss–Seidel type iterations. For quasilinear systems the method of Ranganath and Clifton [5] proved its usefulness.

(3) Much more experimental data is needed to test the usefulness of these and other constitutive hypotheses. The same material should be tested with different incremental loadings after varying amounts of prestrain, and alternative strain recording techniques should be used. There is some evidence that strain gages lag behind as they approach the maximum in a dynamic plastic strain pulse; see, for example, Sharpe[10]. Perhaps optical methods (Bell[11] or Sharpe[12]) could be used to advantage to compare with the strain-gage results. It seems unlikely, however, that the large differences between the experiment and the theories can all be attributed to lag in the strain gage response.

Acknowledgements—The integro–differential formulation discussed in this paper was conceived and given a specific form by Dr. Ion Suliciu, whose help is sincerely acknowledged. Financial support for the work reported here was provided by NSF grant No. GK-23452.

REFERENCES

1. C. H. Yew and H. A. Richardson, Jr., The strain rate effect and the incremental plastic wave in copper, *Exp. Mech.* **9**, 366–373 (1969).
2. L. E. Malvern, The propagation of longitudinal waves of plastic deformation in a bar of material exhibiting a strain-rate effect, *J. Appl. Mech.* **18**, 203–208 (1951).
3. G. Bianchi, Some experimental and theoretical studies on the propagation of longitudinal plastic waves in a strain-rate-dependent material, *Stress Waves in Anelastic Solids*, edited by H. Kolsky and W. Prager, pp. 101–117. Springer, Berlin (1963).
4. N. Cristescu, A procedure for determining the constitutive equations for materials exhibiting both time-independent and time-dependent plasticity, *Int. J. Solids Struct.* **8**, 511–531 (1972).
5. S. Ranganath and R. J. Clifton, A second order accurate difference method for systems of hyperbolic partial differential equations, *Comp. Meth. in Appl. Mech. and Engr.* **1**, 173–188 (1972).
6. P. Perzyna, The constitutive equations for rate-sensitive materials, *Quart. Appl. Math.* **20**, 321–332 (1962).
7. N. Cristescu, *Dynamic Plasticity*. North Holland, Amsterdam; and John Wiley, New York (1967).
8. A. K. Banerjee, *Plastic stress waves in prestressed thin-walled tubes: Numerical Analysis by rate-dependent theories*, Ph.D. Dissertation, University of Florida (1972).
9. N. Cristescu, The unloading in symmetric longitudinal impact of two elastic-plastic bars, *Int. J. Mech. Sci.* **12**, 723–738 (1970).
10. W. N. Sharpe, Jr., Dynamic plastic response of foil gages, *Exp. Mech.* **10**, 408–414 (1970).
11. J. F. Bell, The physics of large deformation of crystalline solids, *Springer Tracts in Natural Philosophy*, vol. 14. Springer, New York (1968).
12. W. N. Sharpe, Jr., Dynamic strain measurement with the interferometric strain gage, *Exp. Mech.* **10**, 89–92 (1970).